Time variabilities of solar wind ion fluxes and of X-ray and EUV emissions from comet Hyakutake

M. Neugebauer[1], T. E. Cravens[2], C. M. Lisse[3,4], F. M. Ipavich[5], R. von Steiger[6], P. D. Shah[2] and T. P. Armstrong[2]

1. Jet Propulsion Laboratory, California Institute of Technology, Pasadena 91109
2. Dept. of Physics and Astronomy, University of Kansas, Lawrence
3. Dept. of Astronomy, University of Maryland, College Park
4. NASA Goddard Space Flight Center, Greenbelt, MD
5. Dept. of Physics, University of Maryland, College Park
6. International Space Science Institute, Bern, Switzerland

Abstract

Observations of X-ray and extreme ultraviolet (EUV) emissions from comet C/Hyakutake 1996 B2 made by the Röntgen X-ray satellite (ROSAT) and the Extreme Ultraviolet Explorer (EUVE) revealed a total X-ray luminosity of about 500 MW. The observed soft X-ray emission varied by a factor of about 2 over a few hours and by a factor of 4 from day to day. In this paper we seek to relate the temporal variability of the measured X-ray/EUV intensities from comet Hyakutake to the variability of the solar wind. Data from the proton monitor of the CELIAS experiment on SOHO are mapped from SOHO to the comet and show that the solar wind proton flux variations do not correlate well with variations in the X-ray/EUV intensities. Although heavy-ion measurements specific to the time and location of the comet Hyakutake observations are not available, Ulysses data are used to demonstrate that at low heliographic latitudes the relative abundance and the flux of high-charge-state oxygen in the solar wind can vary greatly from day to day. The statistical evidence leads us to conclude that sufficient temporal variability exists in the heavy ion fluxes in the solar wind to account for the observed variations in the cometary X-ray and EUV intensities in agreement with the solar wind charge transfer mechanism proposed by Cravens. Although a connection between cometary X-ray/EUV outbursts and encounters with the heliospheric current sheet cannot be ruled out in the case of comet Hyakutake, such a connection is unlikely for an EUV outburst from comet Encke because the current sheet was >10° north of the comet at the time of the outburst.

1. Introduction

The emission of X-rays and extreme ultraviolet (EUV) radiation by active comets is now well established [*Lisse et al.*, 1996; *Dennerl et al.*, 1997; *Mumma et al.*, 1997; *Owens et al.*, 1998; *Lisse et al.*, 1999]. Although several different mechanisms for the generation of this energetic radiation have been suggested [*Lisse et al.*, 1996; *Bingham et al.*, 1997; *Ip and Chow*, 1997; *Krasnopolsky*, 1997; *Northrop et al.*, 1997], the most promising one is the charge-transfer mechanism proposed by *Cravens* [1997]. This process involves charge-exchange collisions between highly charged heavy ions in the solar wind with neutral gas in the cometary coma, resulting in excited ions in lower charge states which radiate in the X-ray and EUV regions of the spectrum. The charge transfer mechanism can explain the X-ray luminosity of comet Hyakutake [*Wegmann et al.*, 1998], the spatial distributions of the X-ray/EUV emissions of a number of comets [*Dennerl et al.*, 1997; *Häberli et al.*, 1997; *Wegmann et al.*, 1998; *Lisse et al.*, 1999], and the low-resolution energy spectra of comets Hyakutake, Levy, and Encke [*Dennerl et al.*, 1997; *Wegmann et al.*, 1998; *Lisse et al.*, 1999].

Another important feature of the observed X-ray and EUV emission is its time variation. The soft X-ray emission observed from comet Hyakutake by ROSAT varied by a factor of about 2 over a few hours and a by factor of ~4 over about a day [*Lisse et al.*, 1996]. As shown in Section 2, the EUV emission from comet Hyakutake was similarly variable. In this paper we seek to relate the temporal variability of the measured X-ray and EUV intensities from comet Hyakutake to the variability of the solar wind using data from the Proton Monitor of the CELIAS experiment on SOHO [*Ipavich and al.*, 1998] and from the Solar Wind Ion Composition Spectrometer (SWICS) on Ulysses [*Gloeckler et al.*, 1992]. The implications for the charge transfer mechanism are discussed in Section 6.

2. Time variations of X-ray and EUV emissions by comet Hyakutake and by the Sun

Lisse et al. [1996] reported on cometary EUV emission measured by the ROSAT wide-field camera (WFC) with an effective spectral range of 90 - 200 eV and on soft X-ray emission measured by the ROSAT high-resolution imager (HRI) with an effective spectral range of 100 eV - 2.0 keV. The ROSAT data are replotted in Figure 1a and can be summarized as follows: the emission (i.e., count rates) on March 27, 1996 is a factor of 2 to 3 greater than the emission on March 26, but within each day another factor of 2 variation was present. The exposure times varied from 897 to 3009 s (0.25 to 0.84 hours).

Figure 1b shows data acquired by the Deep Space Lexan detector on the near-Earth EUVE satellite (described in [*Bowyer and Malina*, 1991; *Sirk et al.*, 1997]). The data were obtained from the EUVE public archive available at http://heasarc.gsfc.nasa.gov/docs/frames/euve_archive.html. The spectral band is 70 to 180 eV and the time resolution is 96 minutes. This panel also shows substantial variations, both over the course of several hours and from day to day.

The Sun is also a variable source of X-rays and EUV radiation which could be reflected by the cometary coma. Figure 1d displays the fluctuations in solar photons in the wavelength band 1 to 770 Å (energy range 16 eV to 12 keV) measured by the Solar EUV Monitor (SEM) on SOHO. The SEM is described in [*Judge et al.*, 1998]. The variations in the cometary x-ray emission appear to be unrelated to the variation in solar x-ray emission. The data in Figure 1 thus confirm the independence of the cometary and solar emissions found by *Lisse et al.* [1999] in their study of comet Encke.

The question addressed in the following sections is whether or not time variations in the X-ray and EUV fluxes from comet Hyakutake can be explained on the basis of the solar wind heavy ion charge transfer mechanism.

3. Solar wind charge transfer mechanism for cometary X-rays and implications for time variations

The solar wind contains heavy-ion species with a range of charge states, such as O^{6+}, O^{7+}, C^{5+}, C^{6+}, N^{5+}, and Si^{10+}. With cross sections at typical solar wind speeds $>10^{-15}$ cm^2 [*Wegmann et al.*, 1998], these ions can readily undergo charge-transfer collisions with cometary neutrals, producing highly excited ions which subsequently emit photons at extreme ultraviolet and X-ray wavelengths. The photon emission rate is proportional to the flux of heavy ions in the solar wind. The EUV and soft X-ray energy emission rate per unit volume (units of $eV/cm^3/s$) for the charge transfer mechanism is given by Equations 2 and 3 in the paper by Cravens. From those equations one can find a simple equation for the photon emission rate (units of $photons/cm^3/s$) as a function of position **r** relative to the cometary nucleus:

$$P(\mathbf{r}) = n_n \, \Phi_{SW} \, \sigma_{eff} \qquad (1)$$

where n_n is the cometary neutral density and Φ_{SW} is the total solar wind ion flux (mainly protons) in the reference frame of the comet. σ_{eff} is an effective cross section (units of cm^2) for soft X-ray/EUV emission which incorporates the abundances of heavy ions in the solar wind relative to protons and their charge states, the charge transfer cross sections, and the branching ratios for emission for transitions leading to photons with energies in the appropriate ranges to be detected by ROSAT and EUVE. The volume emission rate, P(**r**), is a function of **r**, as are all the variables on the right-hand side of Equation 1. The integral of P(**r**) over the complete volume of the emitting region of the cometary coma gives the total X-ray/EUV photon production rate, Q_{photon} (units of s^{-1}):

$$Q_{photon} = Q_{gas} \, \Phi_{SW} \, \langle \varepsilon \rangle \qquad (2)$$

where Q_{gas} is the total neutral gas production rate of the comet. The product $Q_{gas} \langle\varepsilon\rangle$ is the integral of $(n_n \sigma_{eff})$ over the cometary volume; for an optically thin case, the integral can be approximated as $\sigma_{eff}\tau$, where τ is the lifetime of a cometary neutral against ionization. $\langle\varepsilon\rangle$ has units of cm^2 s and is a coma-averaged efficiency function which strongly depends on the solar wind heavy ion composition, including the charge state distribution.

Note that some other suggested cometary X-ray production mechanisms (e.g., electron bremsstrahlung, [*Bingham et al.*, 1997; *Northrop et al.*, 1997]) should also depend on the variables Q_{gas} and Φ_{SW}, although not necessarily in such a simple linear manner. *Dennerl et al.* [1997] used data from several comets from the ROSAT all-sky survey to demonstrate that the X-ray luminosity of comets increases with the cometary gas production rate, Q_{gas}, but *Lisse et al.* [1999] found a dependence on $Q_{gas}^{1/2}$ rather than direct proportionality. *Dennerl et al.* [1997] also showed that the peak X-ray surface brightness varies from comet to comet as the inverse square of the heliocentric distance of those comets (with some additional dependence on the dust-to-gas ratio of the comet). The solar wind flux also varies as the inverse square of the heliocentric distance, on the average, so that this observational fact is also consistent with Equation 2. The factor of ~2 variability in addition to the heliocentric distance dependence could be related to the temporal variability of the solar wind.

4. Correlations between solar wind proton flux and X-ray/EUV emission

In the flux-transfer model, the X-ray luminosity of a comet should be proportional to the solar wind flux, Φ_{SW}, according to Equation 2, provided that the parameters Q_{gas} and $\langle\varepsilon\rangle$ remain constant. The solar wind was observed during the time of the ROSAT and EUVE observations of comet Hyakutake by spacecraft near Earth and by SOHO which is ~1.5×10^6 km sunward of Earth in a halo orbit about the L1 Earth-Sun Lagrangian point. The near-Earth spacecraft measured the solar wind protons and alpha

particles and the magnetic field, but had no instrumentation for measuring the fluxes of minor heavy ions. Hourly averages of near-Earth data compiled from the observations of a number of different spacecraft are available via the World Wide Web from the National Space Science Data Center OmniWeb. Although the SOHO/CELIAS experiment is capable of measuring the fluxes of highly charged heavy ions, that particular part of the experiment (CTOF) was not operating at the time of interest; furthermore, SOHO has no magnetometer. Thus this part of our study is limited to the properties of protons measured by the SOHO/CELIAS Proton Monitor with a 5-minute time resolution and hourly averages of plasma properties from OmniWeb.

Figure 2 displays several properties of the solar wind observed near Earth and at SOHO for the period of interest. From top to bottom, the panels in this figure are: the proton speed in km/s, the proton density in cm^{-3}, the proton flux in units of 10^8 cm^{-2} s^{-1}, the longitudinal and latitudinal directions of the solar wind flow vector in degrees, and the azimuthal angle of the interplanetary magnetic field in degrees. This last parameter is included to show that there were no crossings of the heliospheric current sheet (also known as a magnetic sector boundary) near Earth during this interval. Figure 2 shows that for the 3.5 days of interest the solar wind proton flux varied by a factor slightly >3. But even though a sufficient level of variability may be present in the solar wind, can it explain the specific time variation of the comet Hyakutake X-ray/EUV data? That is, is the solar wind flux correlated with the X-ray/EUV counting rates?

To answer those questions, we must extrapolate or map the data acquired near Earth to the position and time of the comet observations. Most significant structure in the solar wind originates at the Sun and is to a large extent frozen into the solar wind moving radially outward at the solar wind speed. Quasi-stationary solar wind structures, but not fluid parcels, also corotate with the Sun. The solar wind conditions at the comet at a given time can be estimated by using solar wind parameters measured near Earth or at SOHO and introducing a time shift which includes both a radial and a corotational component. We cannot account for and therefore must neglect

any latitudinal structure that might be present in the solar wind. The radial time shift is

$$\Delta t(\text{radial}) = \Delta r \,/\, (u_{sw} + 36\ \text{km/s}) \qquad (3)$$

where Δr is the difference in the heliocentric distances of the comet and Earth or SOHO and 36 km/s is the inward velocity component of the comet relative to the Earth and SOHO. Positive values of Δt and Δr are defined such that the solar wind hits the Earth and SOHO before it hits the comet. That is, the solar wind parameters for $\Delta t(\text{radial}) > 0$ should be sampled near Earth or at SOHO at a time earlier than the comet observations.

The corotation (or longitudinal) time shift depends on the difference between the heliographic longitudes of the comet and the Earth or SOHO:

$$\Delta t(\text{longitudinal}) = \Delta\phi \,/\, \Omega \qquad (4)$$

where $\Omega = 2\pi/T_s$ is the rotational frequency of the Sun. T_s is the Sun's rotation period (in the Earth's and SOHO's frame of reference) = 27 to 28 days; a period of 28 days was used in our calculations, but the results are very insensitive to the exact value used. $\Delta\phi$ is the difference in the heliolongitudes of the comet and Earth or SOHO. The Earth and SOHO were always ahead of the comet so that the corotating solar wind always encountered the comet's longitude before it encountered the longitude of Earth/SOHO. The net time shift between SOHO and the comet,

$$\Delta t = t_{comet} - t_{SOHO} = \Delta t(\text{radial}) + \Delta t(\text{longitudinal}) \qquad (5)$$

is plotted in Figure 3. Its calculation was based on the comet ephemeris, the SOHO trajectory, and the speed of the solar wind observed by SOHO. The minor wiggles in Δt are caused by variations in solar wind speed. Δt ranged from ~4 hours positive to ~12 hours negative. Also shown in Figure 3 is the difference in the heliographic latitudes of the comet and SOHO.

Figure 1c shows the proton flux, Φ_p, measured by SOHO delayed/advanced by Δt according to Equations 3 to 5. Φ_p is the solar wind proton flux in the reference frame of the comet; $\Phi_p = n_p(v_p + 36\ km/s)$, where n_p and v_p are the density and speed of solar wind protons. The SOHO measurements of Φ_p with 5-min resolution were mapped to the comet and then averaged over the 96-min duration of the EUVE measurements.

Comparison of the top three panels in Figure 1 reveals good correlation of the ROSAT and EUVE data (Panels a and b) with each other but poorer agreement between the proton flux and the X-ray/EUV emission. If one removes the data for March 26.5 through March 27.5, the correlation coefficient between the EUV and proton fluxes is 0.45, which is still rather poor. But a more severe problem is the large peak in the proton flux early on March 27 for which there is no corresponding X-ray/EUV enhancement.

We can think of no mechanism for shifting the time of arrival of the high-flux stream at the comet by ~0.7 days so that it aligns with the X-ray and EUV peaks on March 27.8. Two possibilities were considered, but both are probably too small. First, solar wind features would arrive at the comet slightly later than given by Equations 3 through 5 because the wind is slowed on its approach to the comet by the pickup of cometary ions. This effect, however, is estimated to be less than an hour. Alternatively, the solar wind might not have been in a corotating quasi-stationary state, but its structures might have been transient and on locally spherical shells. In that case, Δt(longitudinal) = 0, the flux structures at the left of Figure 1c would arrive up to 0.3 days later, those on March 28 would arrive ~0.1 day earlier, and the profiles of the two flux peaks on March 27 would change hardly at all.

Figure 2 shows an abrupt change in the flow longitude angle and the start of a slower change in the flow latitude angle at the time of the steep density and flux decreases in the middle of March 27, so it is possible that the solar wind shifted directions such that the stream with high proton flux missed the comet. There have been several studies of the accuracy of mapping solar wind features from one location to another. For one example, *Richardson et al.* [1998] compared measurements by ISEE 3 near L1 with near-

Earth measurements by IMP 8 with time lags (Δt) of 30 to 60 minutes, and found an average correlation coefficient for the proton fluxes of ~0.6, but when there were large temporal variations in the flux such as those seen in Figure 2, the correlation coefficient rose to 0.85. The fact that both SOHO and the near-Earth spacecraft saw the same increase in flux on March 27 makes it unlikely that the high-flux stream missed the comet unless that stream did not extend over the ~6° latitude difference between Earth/SOHO and the comet. Although we know of no study of small scale latitudinal gradients of solar wind flux, in equatorial regions, latitudinal gradients in solar wind speed are known to range from 10 to 100 km/s/deg (see discussions by *Miyake et al.* [1989] and *Gazis* [1993] and Ulysses observations by *Neugebauer et al.* [1998]). In Section 6 we speculate further on possible reasons for the poor correlation between proton and X-ray/EUV fluxes and the implications for the charge-transfer mechanism.

5. Time variation of solar wind composition

The analysis in the previous section presumed that variations in the abundance of heavy ions relative to protons, included in the parameter $<\varepsilon>$ in Equation 2, are negligible compared to variations in the total solar wind or proton flux. There are two types of variations in the heavy ion flux: compressions/rarefactions in the interplanetary medium and intrinsic variations related to the different sources of the solar wind streams. The first type is caused by interactions of fast and slow streams of plasma in interplanetary space and affects only the local flux, not the elemental abundances or charge states of the ions. This type of variation is well tracked by the proton flux discussed in the previous section. The second type, the intrinsic abundance variations, could not be studied with data available from spacecraft close to comet Hyakutake. For this second type, we therefore investigate the temporal variability of heavy ion abundances observed in the solar wind by the SWICS instrument on Ulysses at other times and places.

Figure 4 illustrates the variability of the oxygen ion abundance during the Ulysses fast latitude scan [*Smith and Marsden*, 1995]. The top panel of the figure shows the change of the spacecraft's latitude with time during that interval. The data in the middle panel are 3-hour averages of the ratio of the flux of O^{6+} and O^{7+} ions (the charge states of nearly all of the oxygen ions) to the flux of protons. The data were acquired between day 358 of 1994 and day 127 of 1995, as Ulysses moved from a heliographic latitude of 49°S at a solar distance of 1.60 AU, through the solar equator on day 62, 1995, at a distance of 1.34 AU, to a latitude of 48°N and a distance of 1.48 AU. One can conclude from the middle panel of Figure 4 that at intermediate and high latitudes (i.e., before ~day 30 and after ~day 95 of 1995) and for some intervals at low latitudes (e.g., days 55 to 60 of 1995), the day-to-day variations in the abundance of oxygen ions are small compared to the X-ray/EUV variability of comet Hyakutake, so that the approximation of a constant value of $<\varepsilon>$ would be justified. There are other intervals at low latitudes, however, that show very significant variations in oxygen ion abundance.

The bottom panel of Figure 4 provides plots of 3-hr averages of the fluxes of O^{6+} and O^{7+} ions observed by Ulysses. Much of the scatter in the O^{7+} flux is caused by poor counting statistics for this relatively rare ion. Figure 5 shows hourly averages of the O^{6+} flux on an expanded time scale for 10-day intervals at intermediate (top panel) and low (bottom panel) latitudes. Since the comet was at a heliographic latitude close to 1°S when the X-ray/EUV observations were made, these variations would be more than sufficient to account for the day-to-day variability of energetic photons from comet Hyakutake. Such was not the case at higher latitudes where the day-to-day variations in the O^{6+} flux were usually less than a factor of 2.

6. Discussion

In the previous sections we used two methods of assessing the consistency of the charge-transfer model with the observed variability of X-ray and EUV emission from comet Hyakutake. In the first method we compared

the proton flux measured on SOHO to the cometary emissions and obtained disappointing results. A high-flux stream was observed both near Earth and at SOHO which had no apparent effect on the comet. This disagreement is probably not fatal for the charge-transfer model, however, for a number of reasons. First, as discussed in Section 4, there are problems mapping the spacecraft data to the comet. The high-flux stream detected at Earth/SOHO may not have reached the latitude of the comet (6° north of Earth). Second, the proportionality between solar wind flux and the X-ray/EUV emission predicted by the charge-transfer model requires that the cometary gas production rate, Q_{gas} in Equation 2, remain approximately constant. The X-ray intensity shown in Figure 1b exhibits a possible modulation with a period close to 6 hours, in agreement with the observed 6.2-hr rotation period of the nucleus [*Schleicher et al.*, 1998]; this modulation is quite small, however, so that $Q_{gas} \approx$ constant is probably a valid assumption over the time period considered. Finally, and perhaps most importantly, the values of σ_{eff} in Equation 1 and $\langle\varepsilon\rangle$ in Equation 2 may not have remained constant. The high-flux stream observed at SOHO in the middle of March 27 may very well have had a lower abundance of heavy ions than did its neighboring streams.

This part of our study of comet Hyakutake parallels a study of comet Encke by *Lisse et al.* [1999]. Like comet Hyakutake, comet Encke exhibited both slow, day-to-day variations in its EUV emission and an impulsive burst of ~3 hours duration with a factor of 3 increase in EUV count rate. As with comet Hyakutake, the cometary outburst did not correlate with solar X-ray emission, but in that case the comet outburst was closely correlated in time with an increase in the proton flux of the solar wind.

It is interesting to compare the possible relation of cometary outbursts to crossings of the heliospheric current sheet (HCS). At the time of the Hyakutake observations, both Earth and SOHO were embedded in an interplanetary magnetic field (IMF) with an inward polarity, which indicates a location to the south of the HCS. Models of the IMF calculated from observations of the magnetic field at the solar surface (available at http://quake.stanford.edu/~wso/coronal.html) place the HCS a few degrees to

the north of Earth/SOHO, consistent with the polarity of the IMF observed near Earth. Because models of the latitudinal location of the HCS are generally accurate within a few degrees [*Neugebauer et al.*, 1998], and because comet Hyakutake was also slightly north of Earth, it is possible that the X-ray/EUV outburst of the comet was associated with the interaction of the HCS with the comet.

With a similar argument we can conclude that the EUV outburst of comet Encke was probably not caused by interaction with the HCS. In that case, the HCS passed from south to north of Earth a few hours before the start of the outburst when comet Encke was 1 AU from the Sun and ~0.18 AU (~10°) south of the Earth [*Lisse et al.*, 1999]. The geometry thus implies that at the time of the Encke EUV outburst, the HCS was north of the Earth, which in turn was ~10° north of the comet, so Encke was almost certainly deeply embedded in the southern magnetic hemisphere well away from the HCS.

Our second approach was to examine the fluxes of O^{6+} and O^{7+} measured by Ulysses; that analysis showed that at the low latitudes at which the comets exhibited X-ray and EUV emissions, the abundance of oxygen ions often varied by an order of magnitude from day to day, as did the fluxes of heavy ions. A corollary is that if the charge-transfer mechanism provides the correct explanation for cometary X-ray/EUV emissions, then there should be no substantial day-to-day variations of cometary X-rays or EUV at high latitudes during the phase of the solar cycle when the high-latitude solar wind emanates from large polar coronal holes. We know of no case in which such high-latitude cometary variations were observed.

7. Conclusions

Because of both latitudinal and compositional variations in the solar wind, cometary emissions do not always correlate well with the solar wind proton flux measured at spacecraft located nearby but removed from the immediate vicinity of the comet. The statistical evidence from Ulysses data leads us to conclude, however, that sufficient temporal variability does exist

in the heavy ion fluxes in the low-latitude solar wind to account for the observed variations in the cometary X-ray and EUV intensities in agreement with the charge-transfer mechanism. Crossing of the heliospheric current sheet is an unlikely cause of cometary X-ray/EUV outbursts.

Acknowledgments. We thank Damian Christian of the EUVE Project at the Space Telescope Science Institute for reducing the EUVE light curve data. M. Mumma was the original Principal Investigator for the EUVE investigation. We also thank S. Ogawa of the University of Southern California for providing the SOHO/CELIAS/SEM solar X-ray data. Part of this research was performed at the Jet Propulsion Laboratory under a contract between the California Institute of Technology and the National Aeronautics and Space Administration. The work at the University of Kansas was supported by NSF under grant ATM 94-23210 and by NASA under grant NAG 5-4358. CML was supported in part by NASA grant NAGW188 and by a cooperative research grant between NASA Goddard Spaceflight Center and the University of Maryland.

References

Bingham, R., J. M. Dawson, V. D. Shapiro, D. A. Mendis, and B. J. Kellet, Generation of X-rays from C/Hyakutake 1996 B2, *Science, 275*, 49, 1997.

Bowyer, S., and R. F. Malina, The Extreme Ultraviolet Explorer Mission, in *Extreme Ultraviolet Astronomy*, edited by R. F. Malina and S. Bowyer, pp. 391, Pergamon Press, New York, 1991.

Cravens, T. E., Comet Hyakutake x-ray source: Charge transfer of solar wind heavy ions, *Geophys. Res. Lett, 24*, 105, 1997.

Dennerl, K., J. Englhauser, and J. Trümper, X-ray emissions from comets detected in the Röntgen X-ray satellite all-sky survey, *Science, 277*, 1625, 1997.

Gazis, P. R., Pioneer Venus and IMP 8 observations of the latitude dependence of the solar wind, *J. Geophys. Res., 98*, 9391, 1993.

Gloeckler, G. L. et al., The solar wind ion composition spectrometer, *Astron. Astrophys. Suppl., 92*, 267, 1992.

Häberli, R. M., T. I. Gombosi, D. L. De Zeeuw, M. R. Combi, and K. G. Powell, Modeling of cometary x-rays caused by solr wind minor ions, *Science, 276*, 939, 1997.

Ip, W.-H., and V. W. Chow, Note: On hypervelocity impact phenomena of microdust and nano X-ray flares in cometary comae, *Icarus, 130*, 217, 1997.

Ipavich, F. M., and e. al., The CELIAS/MTOF proton monitor, *J. Geophys. Res., 103*, 17205, 1998.

Judge, D. L. et al., First solar EUV irradiances from SOHO by the CESIAS/SEM, *Solar Phys., 177*, 161, 1998.

Krasnopolsky, V. A., On the nature of soft-x-ray radiation in comets, *Icarus, 128*, 368, 1997.

Lisse, C. M., D. Christian, K. Dennerl, M. Desch, J. Englhauser, F. E. Marshall, R. Petre, S. Snowden, and J. Trümper, X-ray and extreme ultraviolet emission from comet P/Encke 1997, *Icarus,* In press, 1999.

Lisse, C. M. et al., Discovery of x-ray and extreme ultraviolet emission from comet C/Hyakutake 1996 B2, *Science, 274*, 205, 1996.

Miyake, W., T. Mukai, K.-I. Oyama, T. Terasawa, K. Hirao, and A. J. Lazarus, Thin equatorial low-speed region in the solar wind observed during the recent solar minimum, *J. Geophys. Res., 94*, 15, 1989.

Mumma, M. J., V. A. Krasnopolsky, and M. J. Abbott, Soft x-rays from four comets observed with EUVE, *Astrophys. J., 491*, L125, 1997.

Neugebauer, M. et al., The spatial structure of the solar wind and comparisons with solar data and models, *J. Geophys. Res., 103*, 14, 1998.

Northrop, T. G., C. M. Lisse, M. J. Mumma, and M. D. Desch, A possible source of the x-rays from comet Hyakutake, *Icarus, 127*, 246, 1997.

Owens, A., A. N. Parmar, T. Oostrbroek, A. Orr, L. A. Antonelli, F. Fiore, R. Schultz, G. P. Tozzi, M. C. Macarone, and L. Piro, Evidence for dust-related X-ray emission from comet C/1995 O1 (Hale-Bopp), *Astrophys. J., 493*, 47, 1998.

Richardson, J. D., F. Dashevskiy, and K. I. Paularena, Solar wind plasma correlations between L1 and Earth, *J. Geophys. Res., 103*, 14619, 1998.

Schleicher, D. G., R. L. Mills, D. J. Osip, and S. M. Lederer, Activity and the rotation period of comet Hyakutake (1996 B2), *Icarus, 131*, 233, 1998.

Sirk, M., J. V. Vallerga, D. S. Finley, P. Jelinsky, and R. F. Malina, Performance of the Extreme Ultraviolet Explorer Imaging Telescopes, *Astrophys. J. Suppl., 110*, 347, 1997.

Smith, E. J., and R. G. Marsden, Ulysses Observations from pole-to-pole: An introduction, *Geophys. Res. Lett., 22*, 3297, 1995.

Wegmann, R., H. U. Schmidt, C. M. Lisse, K. Dennerl, and J. Englhauser, X-rays from comets generated by energetic solr wind particles, *Planet. Space Sci., 46*, 603, 1998.

Figure Captions

Figure 1. (a) Soft X-ray and EUV emission detected from comet Hyakutake by ROSAT, from Figure 5 of *Lisse et al.* [1996]. (b) The EUVE flux from comet Hyakutake observed with the EUVE spacecraft. (c) The proton flux observed by the proton monitor on the SOHO spacecraft shifted in time to account for the radial and longitudinal separations of SOHO from the comet. (d) Solar EUV flux observed by the SOHO CELIAS/SEM from 1 to 770 Å.

Figure 2. From top to bottom: solar wind speed (km/s), proton density (cm^{-3}), proton flux (10^8 cm^{-2} s^{-1}), solar wind flow direction in the ecliptic plane (deg), north-south flow direction (deg), and the azimuthal direction of the interplanetary magnetic field (deg). Hourly averages of parameters measured near Earth are plotted as circles and 5-minute averages of parameters measured by the proton monitor on SOHO are plotted by a line connecting consecutive values.

Figure 3. $\Delta t = t_{comet} - t_{SOHO}$, in hours, and $\Delta\lambda = \lambda_{comet} - \lambda_{SOHO}$ = difference in latitude of SOHO and the comet, in degrees, as a function of the time of the observations of the solar wind at SOHO in late March, 1996.

Figure 4. (Top) The heliographic latitude of the Ulysses spacecraft during the fast-latitude scan in early 1995. (Middle) The abundance of O^{6+} and O^{7+} ions relative to protons observed by Ulysses during that time. (Bottom) The fluxes of O^{6+} and O^{7+} ions, where the O^{6+} flux has been multiplied by a factor of 10 for clarity. The average uncertainty due to counting statistics in the O^{6+} flux is ±4% while that in the O^{7+} flux is ±24%. The time resolution is three hours.

Figure 5. Flux of O^{6+} ions observed by Ulysses, as in Figure 4, but with 1-hour time resolution and on an expanded time scale for two 10-day time intervals when the spacecraft was at high (35.5 to 42.3° N, in upper panel) and low (18.4 to 10.9°S, in bottom panel) latitudes.

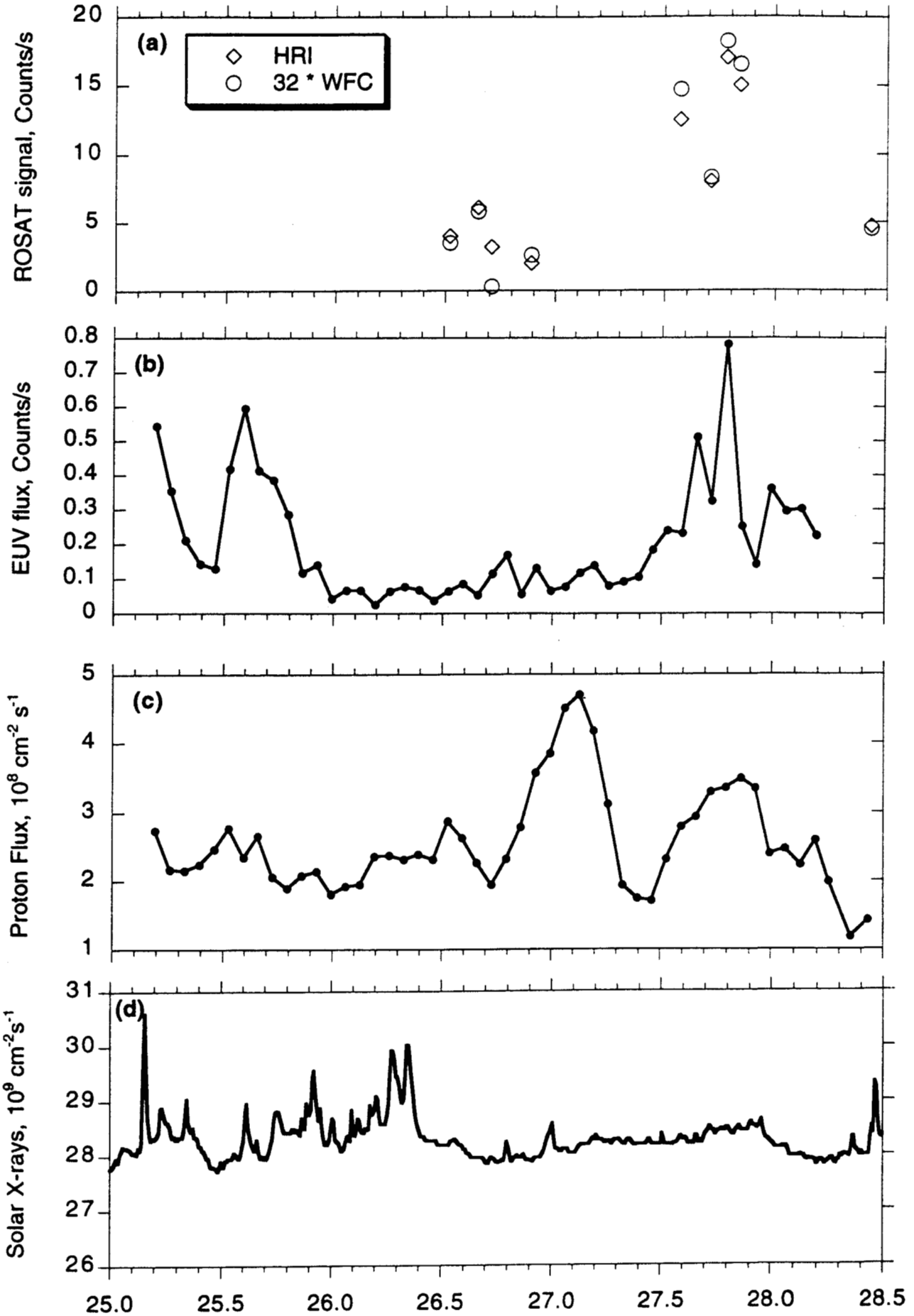
(a)
HRI
32 * WFC
ROSAT signal, Counts/s
20
15
10
5
0
(b)
EUV flux, Counts/s
0.8
0.7
0.6
0.5
0.4
0.3
0.2
0.1
0
(c)
Proton Flux, 10^8 cm^{-2} s^{-1}
5
4
3
2
1
(d)
Solar X-rays, 10^9 cm^{-2}s^{-1}
31
30
29
28
27
26
25.0
25.5
26.0
26.5
27.0
27.5
28.0
28.5
Date, March, 1996

Figure 1

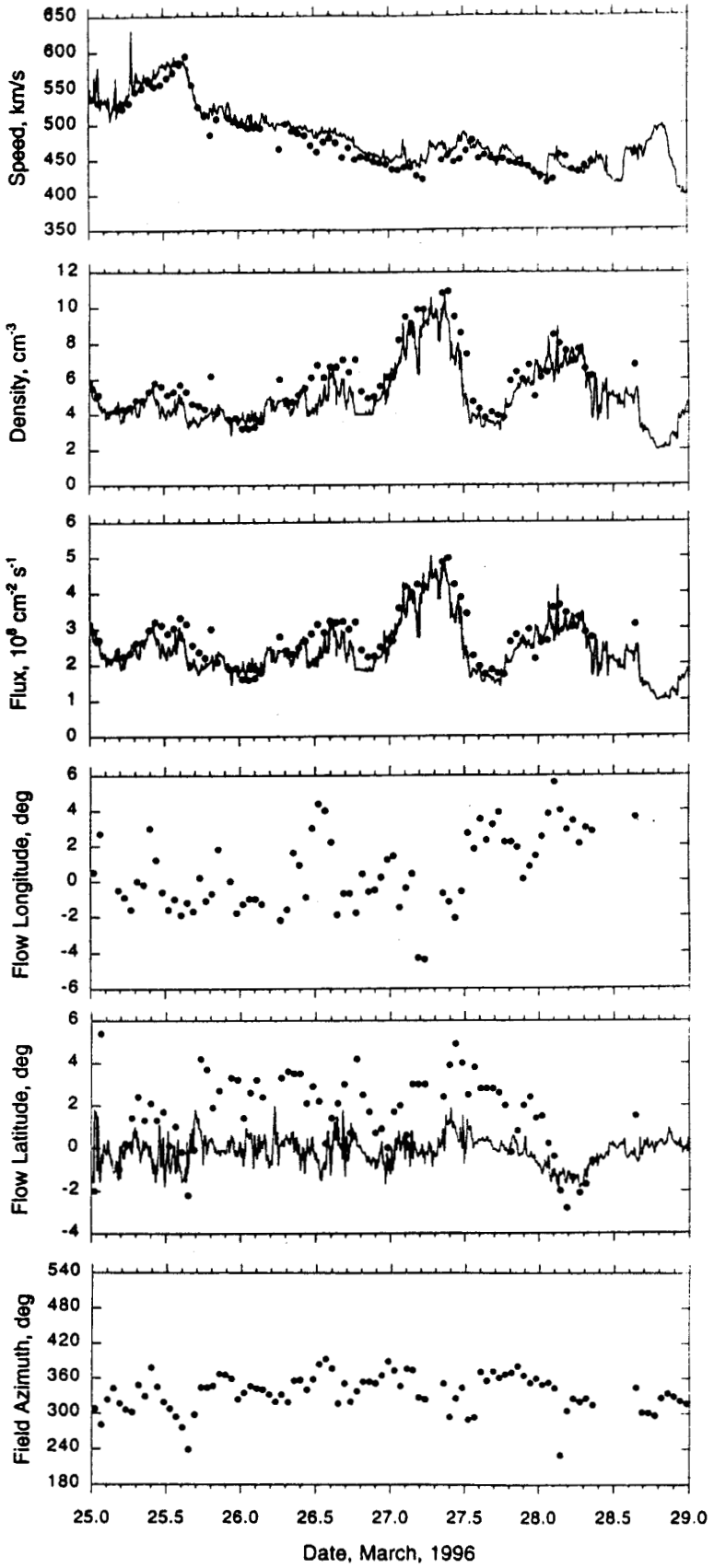
Speed, km/s
650
600
550
500
450
400
350
Density, cm^{-3}
12
10
8
6
4
2
0
Flux, 10^8 cm^{-2} s^{-1}
6
5
4
3
2
1
0
Flow Longitude, deg
6
4
2
0
-2
-4
-6
Flow Latitude, deg
6
4
2
0
-2
-4
Field Azimuth, deg
540
480
420
360
300
240
180
25.0
25.5
26.0
26.5
27.0
27.5
28.0
28.5
29.0
Date, March, 1996

Figure 2

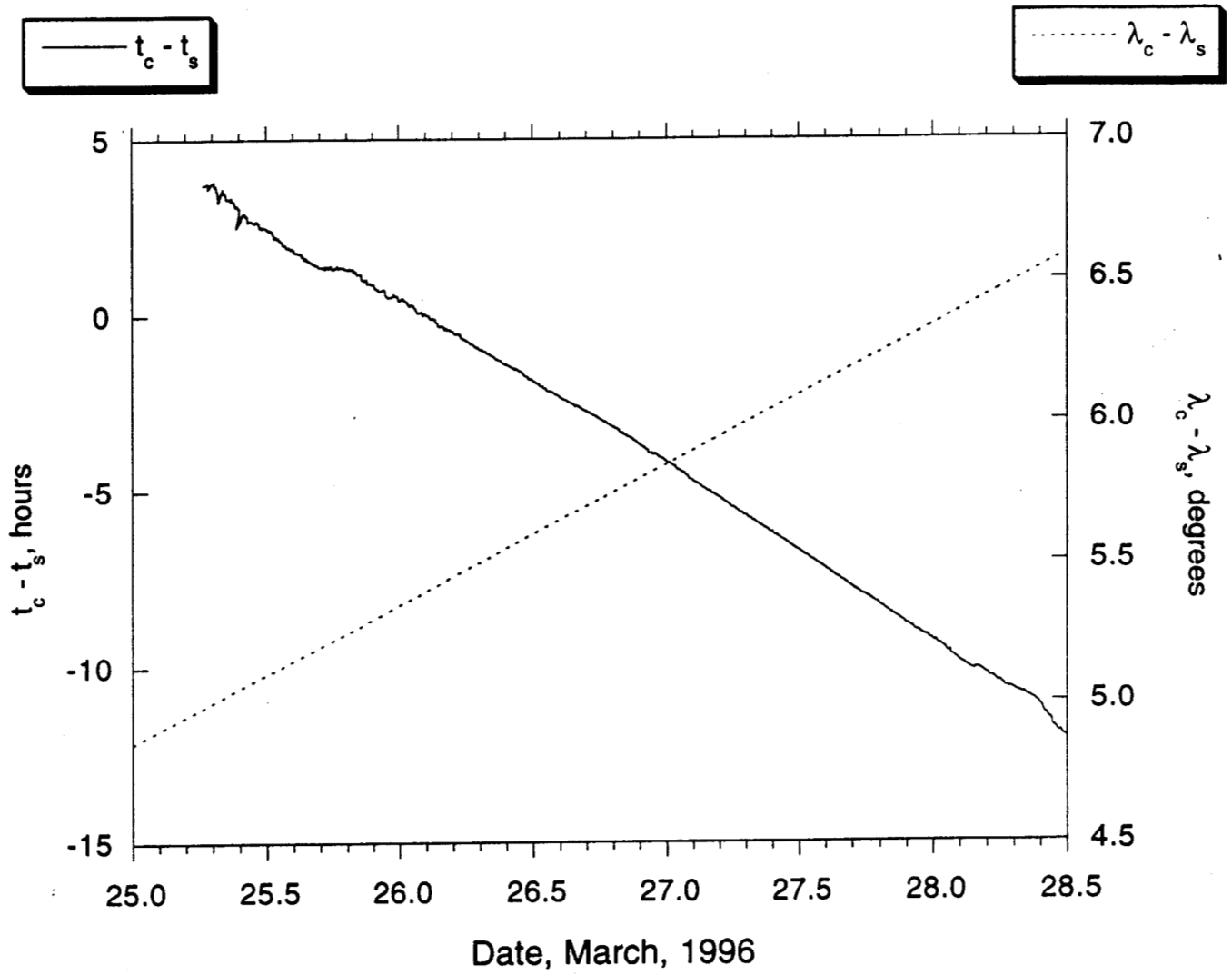
$t_c - t_s$
$\lambda_c - \lambda_s$
5
0
-5
-10
-15
7.0
6.5
6.0
5.5
5.0
4.5
$t_c - t_s$, hours
$\lambda_c - \lambda_s$, degrees
25.0
25.5
26.0
26.5
27.0
27.5
28.0
28.5
Date, March, 1996

Figure 3

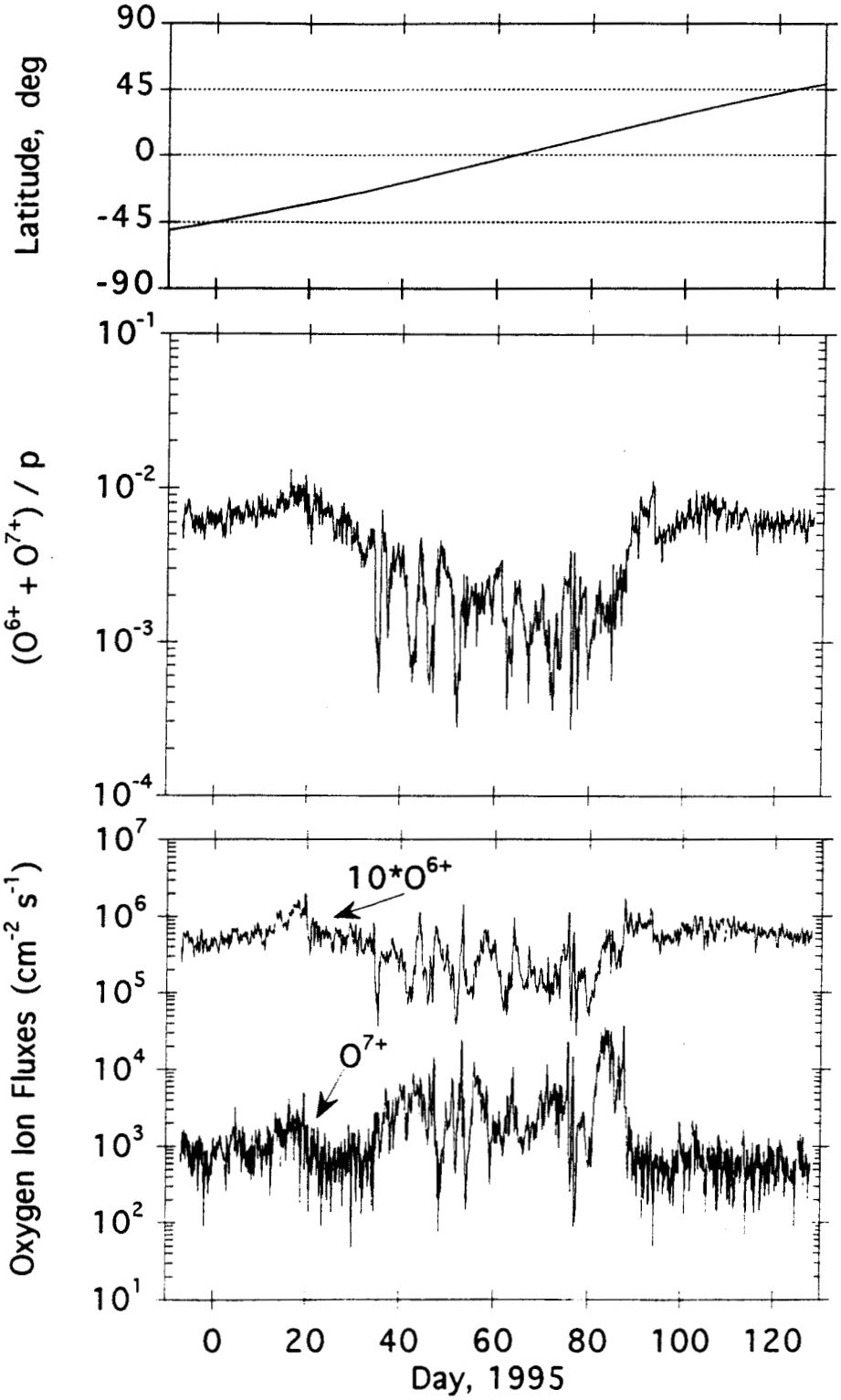
Latitude, deg
90
45
0
-45
-90
$(O^{6+} + O^{7+}) / p$
10^{-1}
10^{-2}
10^{-3}
10^{-4}
Oxygen Ion Fluxes (cm^{-2} s^{-1})
10^{7}
10^{6}
10^{5}
10^{4}
10^{3}
10^{2}
10^{1}
$10*O^{6+}$
O^{7+}
0
20
40
60
80
100
120
Day, 1995

Figure 4

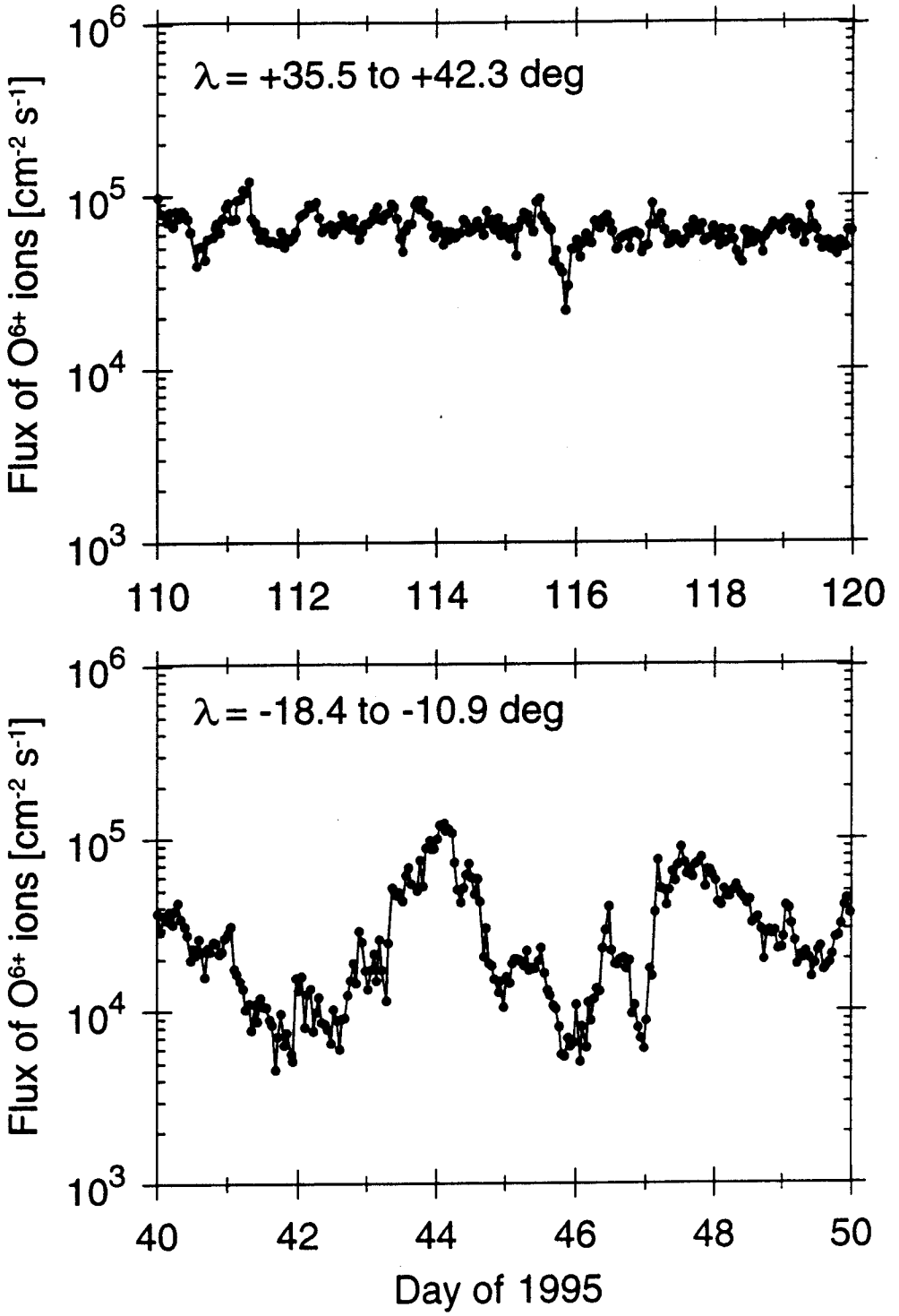
λ = +35.5 to +42.3 deg
λ = -18.4 to -10.9 deg
Flux of O6+ ions [cm-2 s-1]
Flux of O6+ ions [cm-2 s-1]
10^6
10^5
10^4
10^3
110
112
114
116
118
120
40
42
44
46
48
50
Day of 1995

Figure 5